



# Inverse design of materials by multi-objective differential evolution



Yue-Yu Zhang<sup>a</sup>, Weiguo Gao<sup>b</sup>, Shiyong Chen<sup>a</sup>, Hongjun Xiang<sup>a</sup>, Xin-Gao Gong<sup>a,\*</sup>

<sup>a</sup> Key Laboratory of Computational Physical Sciences (Ministry of Education), State Key Laboratory of Surface Physics, and Department of Physics, Fudan University, Shanghai 200433, PR China

<sup>b</sup> School of Mathematical Science, Fudan University, Shanghai 200433, PR China

## ARTICLE INFO

### Article history:

Received 25 August 2014

Received in revised form 21 October 2014

Accepted 28 October 2014

Available online 19 November 2014

### Keywords:

IM<sup>2</sup>ODE

Inverse design

Multi-Objective Differential Evolution

Electronic structure

Hardness

## ABSTRACT

Inverse design is a promising approach in the realm of material science for finding structures with desired property. We developed a new package with novel algorithm for inverse design named as IM<sup>2</sup>ODE (inverse design of Materials by Multi-Objective Differential Evolution). The target properties of concern include the optical and electronic-structure properties of semiconductors, hardness of crystals, etc. IM<sup>2</sup>ODE can easily predict the atomic configurations with desired properties for three dimensional structure, interface and cluster, even complex defect in solid. Tests have been run on multiple systems and it has been proved that IM<sup>2</sup>ODE is highly efficient and reliable, which can be applied widely.

© 2014 Elsevier B.V. All rights reserved.

## 1. Introduction

Traditionally discovering new materials is a long and costly process including a huge amount of trial and error in the progress of synthesizing and testing. Theoretical designing of materials has been a long standing dream of the scientists. With the development of supercomputers and first principle methods, one can correctly predict most of the properties of a material if the atomic configuration is known. However, the inverse of this approach, finding a material with unknown structure and desired properties, is still a great challenge in material design.

One way to do inverse design is by scanning databases of structures previously found and substituting elements in those structures, which is known as ‘high-throughput’ (HT) computational materials design, focusing on finding different composites of compounds [1–7]. Another way is to figure out the atomic configuration of a fixed chemical system with the desired properties, which is often achieved by combining an atomic structure searching with first principle calculations of target properties. These methods were first proposed by Franceschetti and Zunger, using simulated annealing algorithm to predict the atomic configuration of Al<sub>0.25</sub>Ga<sub>0.75</sub>As alloy with the largest optical band gap [8]. Later, genetic algorithm [9,10] and particle swarm optimization [11,12] are proposed to design ordered alloy and meta stable crystal phase with target electronic-structure property. However, these methods take desired properties into account while neglecting the total

energy and it is possible that the structures found by those methods may have rather high energy.

Atomic structure is the most fundamental properties of materials. In the past two decades, quite a few global optimization methods were developed to search the atomic structures [13–17]. Some global optimization packages, such as USPEX [18] and CALYPSO [19], were developed to predict new crystal structures with lowest enthalpy at given external conditions (e.g., pressure). The process of structure prediction involves exploring the energy surface which involves a huge number of energy minima. Highly efficient and robust global optimization methods are applied to solve this problem for sampling the energy surface and find global minima. There is something in common between the structure prediction and inverse design: both of them needs to scan the energy surface. The key difference is that structure prediction only needs to find a structure with the lowest energy, while inverse design needs to find a structure with desired properties.

Based on global optimization methods, we have developed a novel method for “inverse design”, which is named as IM<sup>2</sup>ODE (inverse design of Materials by Multi-Objective Differential Evolution). In this code package, Multi-Objective optimization methods are applied to predict structures with respect to both total energy and properties. By extending the inverse design problem from the single-objective domain to the multi-objective domain, we are able to predict metastable structures of desired properties with relatively low energy. Among the numerous global optimization algorithms, Multi-Objective Differential Evolution (MODE) has been widely used and achieved great successes [20–22]. MODE is

\* Corresponding author.

based on Differential Evolution (DE), which is an evolutionary algorithm that optimizes an objection function by maintaining a population of candidates and creating new ones through mutation and crossover operations based on the differentials of the existing ones [23,24]. Greedy strategy is taken by the algorithm only keeping new candidates which out-perform the old ones. The evolutionary nature of the DE algorithm makes it a very effective solver for complex search problems, including either global or multi-objective problems, have already been applied for structure searching of cluster and interface [25,26]. Therefore MODE algorithm is suitable to be applied to the inverse material design problem.

This rest of the paper is organized as follows. In Section 2, the detailed description of IM<sup>2</sup>ODE code is presented. In Section 3, some applications and tests of the method are given, followed by the conclusion in Section 4.

## 2. Algorithm

Different from the well-known structure search which is essentially single objection optimization, the nature of inverse material design is a multi-objective optimization. For instance, if we want to find suitable material for solar absorber, at least both band gap and total energy should be set as criteria. Therefore a multi-objective optimization method is necessary and here we adopt MODE algorithm. Generally, IM<sup>2</sup>ODE package can be also applied to single objective problem, such as finding the most stable structure of complex systems of clusters on surfaces and interface of crystals. There are mainly four steps in the IM<sup>2</sup>ODE code package: (i) generation of atomic structures, such as two-dimensional material, cluster, surface, interface or defect; (ii) local optimization of structures; (iii) sorting the structures in the solution space and finding duplicate structures; (iv) generation of new structure by DE or MODE operations. The main procedure of IM<sup>2</sup>ODE package is shown in Fig. 1.

### 2.1. Generation of structure

Here we perform inverse design of materials including crystal, two-dimensional material, cluster, surface, interface and defect [16,18,27–30]. In the multi-dimensional search problem, an individual crystal structure is defined as a vector of dimension  $3N + 6$ , which contains six lattice parameters, including three angles and three vectors, and  $3N$  atomic coordinates of  $N$  atoms. The crystal structures are initialized considering the symmetry of the 230 space groups. The definition of two-dimensional materials is similar to that of crystal, and the only difference is that constrain is applied on the third dimension. There are three modes to initialize cluster, which are ball, shell and plate. To design the adsorption of cluster on solid surface, we place a surface below randomly generated cluster to obtain the best configuration of cluster, which dimension is the same as cluster. The interface is simulated with a slab model, containing fixed layer, rigid layer and optimized layer. The rigid layer can move as a whole and the atoms inside the interface are allowed to move for optimization. The dimension of the vector of interface is  $3N + 3$ , which contains the atomic coordinates of the  $N$  atoms and the movement of the rigid layer [25].

### 2.2. Structural optimization

In principle, one can use any method for the structure optimization. Presently, we adopt Ab initio package VASP (Vienna ab initio simulation package) [31] to perform structure optimization and electronic structure calculation, of course we have successfully use classical potentials to perform the structural optimization of large system such as the structural search of grain boundary in graphene. In order to increase the efficiency, atomic coordinates and lattice parameters of the structures are locally optimized after initialization which can reduce the noise in the complex searching space and simplify the task of finding the global minimum on the

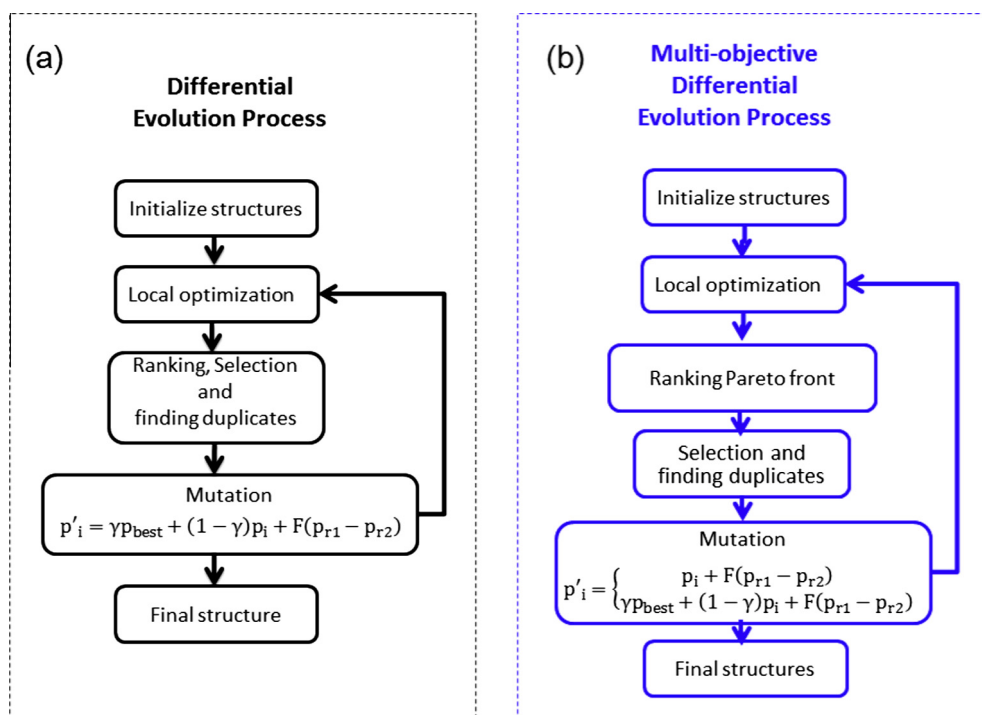


**Fig. 1.** Procedure of the IM<sup>2</sup>ODE package including both DE process for single objective optimization (a) and MODE for multi-objective optimization (b). In the initialization step, crystal, two-dimensional material, cluster, surface, interface and defect can be generated. After that, local optimization of structures, ranking, selection, and mutation are performed iteratively until a predefined generation is reached and finally find out the optimized structure.

energy landscape [18]. As soon as the ground state structure is reached, the physical properties such as electronic band structures and bulk modulus can be calculated by conventional first principal method.

### 2.3. Eliminating duplicates

In order to increase the efficiency of the IM<sup>2</sup>ODE package, we eliminate similar structures in the optimization progress. The total Euclidean distance between two structures is defined as the similarity of the two structures. If the Euclidean distance is less than a certain criteria, one of the structures will be eliminated. To calculate the Euclidean distance, two structures  $X$  and  $X'$  are modeled as a bipartite graph, whose vertices can be divided into two disjoint sets  $U$  and  $V$  such that every edge connects a vertex in  $U$  to one in  $V$ . The position of atoms in structure  $X$  are put into  $U$  and that of structure  $X'$  into  $V$ , which are two disjoint sets. Distance of atoms of the same kind can be represented by edges connecting them. A bipartite graph  $G_{XX'}$  of structure  $X$  and  $X'$  can be defined as a triple  $(U, V, E)$ , where  $U$  is a set of atoms in structure  $X$ ,  $V$  is a set of atoms in structure  $X'$ ,  $E$  is distance between atoms in  $X$  and  $X'$ :  $E = \{(x, x') | x \in X, x' \in X'\}$ . The smallest total distance between  $X$  and  $X'$  can be solved by Kuhn–Munkres algorithm [32]. If the total distance is below a certain criteria, one of the structures will be eliminated. The test shows that the present algorithm is very efficient.

### 2.4. Single-objective optimization

Single-objective optimization is implemented in our package, and IM<sup>2</sup>ODE can be easily adopted to perform structure prediction if the total energy is used as the objective. As optimizing atomic structure is a continuous optimization problem, we adopt DE algorithm to perform global optimization [33]. After the generation of initial structures, the algorithm enters a loop of ranking, selecting, and creating the next generation until a pre-defined generation is reached, which is illustrated in Fig. 1(a). The selection operator is to keep the top 60% solutions and the rest are replaced by newly generated solutions. The following mutation operator is applied to generate offspring:

$$p'_i = \gamma p_{\text{best}} + (1 - \gamma)p_i + F(p_{r1} - p_{r2}) \quad (1)$$

where  $p_i$  is a vector which represents a solution in the parent population,  $p_{\text{best}}$  is the best solution in the parent population,  $p_{r1}$  and  $p_{r2}$  are randomly selected from the parent population which are distinct,  $\gamma \in [0, 1]$  and  $F \in [0, 1]$  are scale factors of the operator.

The objective can be set as the total energy to find the most stable structure for all of the systems mentioned above such crystal, cluster and interface, and can also be set as band gap or bulk modulus.

### 2.5. Multi-objective optimization

Here we combine the multi-objective with DE algorithm in the IM<sup>2</sup>ODE package to perform multi-objective optimization for inverse design. The MODE algorithm is a kind of multi-objective evolution algorithm which has been successfully applied in a wide range of applications [20–22,34–36]. Following the general concept of evolutionary algorithms, MODE starts with a population of  $N_p$ , and finally finds a set of solution on the first Pareto front through iterations, which contains local optimization, ranking the Pareto front, selection and mutation, as is shown in Fig. 1(b). Each of the population is presented as a vector as described above to present the structural information of materials.

#### 2.5.1. Ranking Pareto front and Selection

In a multi-objective problem, the objective can be defined as

$$\min Z(x) = [z_1(x), z_2(x), \dots, z_k(x)], \quad (2)$$

where  $x$  is the decision variables (the structural parameters in IM<sup>2</sup>ODE package), and  $z_i(x)$  is the objective function. The definition of dominate is: a vector  $Z(x)$  is dominating another different vector  $Z'(x)$ , which is denoted as  $Z(x) < Z(x')$ , if and only if  $z_i(x) \leq z_i(x')$  for all  $i \in \{1, 2, \dots, k\}$ . A solution  $x$  is on the Pareto front if and only if there is no solution  $x'$  that dominates  $x$ . All the non-dominated solutions form the first Pareto front.

The ranking scheme of the Pareto front is as the following [37]: sort all the solutions in the solution space and find those non-dominated to form the first Pareto front. Remove the first Pareto front and repeat the process until there is no solution in the search space.

The selection operation is based on a greedy strategy: an offspring is placed into the population if and only if it dominates its main parent [20]. In order to keep the diversity of the population in IM<sup>2</sup>ODE, only 60% of the structures are kept after ranking and the rest are newly generated. The selection operation is performed after local optimization of the structures.

#### 2.5.2. Mutation

The major operation in MODE to generate new structures is mutation. There are two parts in the mutation operator: differential vector and perturbation vector. The differential operation helps the algorithm to learn from the searching experience, and the perturbation operation prevents the algorithm to be trapped in a local minima. When a solution  $p_i$  is dominated, a quasi-best solution  $p_{\text{best}}$  will be chosen randomly from the first Pareto front of the parent population. The differential vector is defined as the difference between  $p_i$  and  $p_{\text{best}}$ . If  $p_i$  is non-dominated, the  $p_{\text{best}}$  will be itself and the differential vector vanishes. The perturbation vector is defined as the difference between a pair of solutions. Each element in a solution of the population will perform the following operation with the mutation probability  $C_r$ . An offspring  $p'_i$  is generated from  $p_i$ , and  $p_i$  is called the main parent of  $p'_i$ .

$$p'_i = \begin{cases} p_i + F(p_{r1} - p_{r2}) & \text{if } p_i \text{ is non-dominated} \\ \gamma p_{\text{best}} + (1 - \gamma)p_i + F(p_{r1} - p_{r2}) & \text{otherwise} \end{cases} \quad (3)$$

where  $\gamma$  and  $F$  are parameters in MODE,  $r_1, r_2 \in [1, N_p]$  are randomly selected and satisfy  $r_1 \neq r_2 \neq i \neq \text{best}$ .

## 3. Tests and applications

### 3.1. Electronic structures

In order to design materials with desired direct band gap, total energy and a function containing a targeted direct band gap  $E_g$  are set as fitness functions for minimization, so the objectives can be defined as

$$\begin{aligned} \min z_1 &= \text{total energy} \\ \min z_2 &= c_1 |E_g - \text{direct gap}| + c_2 |\text{direct gap} - \text{indirect gap}| \end{aligned} \quad (4)$$

where  $c_1$  and  $c_2$  are parameters.

To test the performance and reliability of the IM<sup>2</sup>ODE package, aluminum oxide ( $\text{Al}_2\text{O}_3$ ) and carbon are chosen for the reason that there are multiple phases with similar total energy but different band gaps. In the  $\text{Al}_2\text{O}_3$  system, if the objective band gap is set as 6.4 eV, IM<sup>2</sup>ODE package would be able to find out  $\alpha\text{-Al}_2\text{O}_3$  within one or two generations with a population of 30 per generation. In the system of carbon, as shown in Fig. 2, if a specific value 4.1 eV is set as the targeted band gap, diamond structure can be found in an average of three generations. If the objective band gap is altered to be 0.0 eV, graphite structure can also be found in three

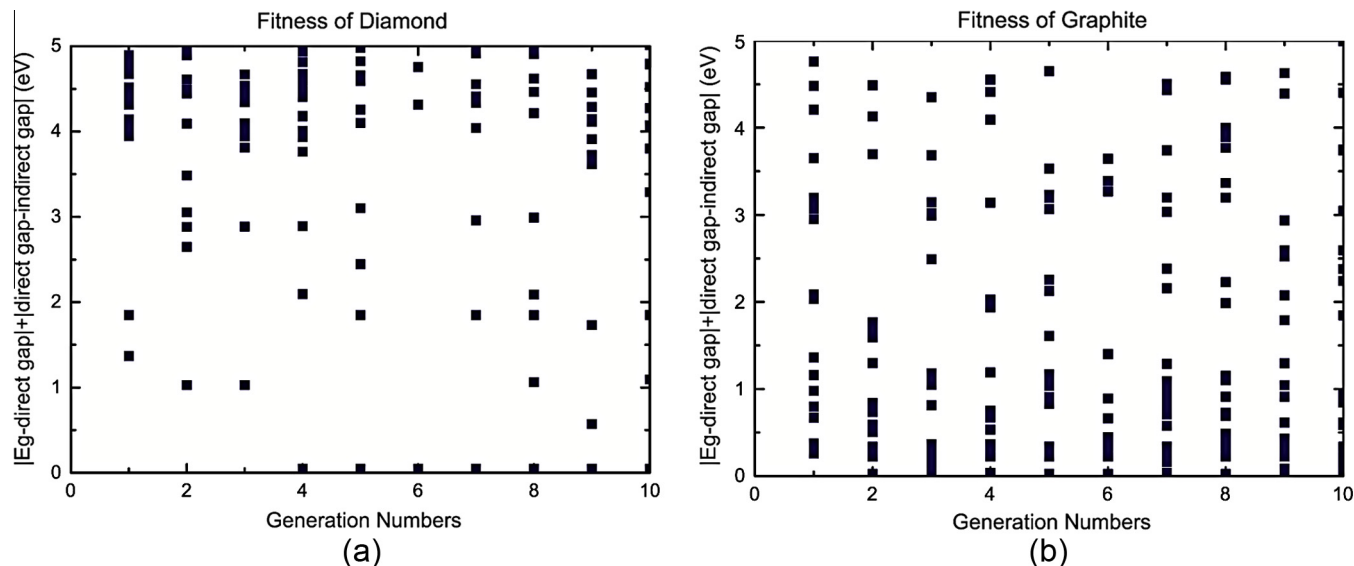


**Fig. 2.** The evolution of objective functions during MODE iterations for diamond (a) and graphite (b). The objective functions are defined in Eq. (4). Diamond structure is found on the fourth generation and graphite is found on the second generation.

steps the same as that in the searching diamond. In all these calculations, the local-density approximation (LDA) is adopted to calculate total energies, relax structures, and estimate band gap.

IM<sup>2</sup>ODE has already been successfully used to predict new TiO<sub>2</sub> polymorphs with better optical absorption ability than that of rutile and anatase [38]. Due to its potential application in solar cell and photo-electrochemical (PEC) water-splitting, TiO<sub>2</sub> has been studied extensively [39–42]. However, the large band gaps of rutile and anatase phase (larger than 3.0 eV) limit its absorption spectra in the ultra-violet region. In order to improve the energy conversion efficiency, IM<sup>2</sup>ODE have been applied to predict new polymorphs of TiO<sub>2</sub> with better optical properties. Two new phases, PI (*pnma*) and CI (C2) are found with band gaps of 1.95 and 2.64 eV, which could be used as high-efficiency solar cell.

### 3.2. Bulk modulus

IM<sup>2</sup>ODE can also be applied to find materials with other desired properties such as large bulk modulus. According to an empirical formula, the objective functions can be written as:

$$\begin{aligned} \min z_1 &= \text{total energy} \\ \min z_2 &= -B = \frac{N_c}{4} \frac{0.624 - 0.070I}{d^{3.5}} \end{aligned} \quad (5)$$

where  $B$  is bulk modulus in GPa,  $d$  is the bond length in nm,  $N_c$  is the average coordination number in the solid, and  $I$  is an ionicity parameter which is zero for Group IV elements, one for III–V compounds, and two for II–VI compounds [43,44].

Carbon nitrides had been extensively studied theoretically and experimentally as an important candidate for super hard materials [45–50]. In the test, we performed multi-objective optimization by Eq. (5) for C<sub>3</sub>N<sub>4</sub> to find out different polymorphs with large bulk modulus. The search was performed with 7 atoms to 28 atoms per unit cell. The number of generation is set as 20 and the population is 30. LDA is applied for structural relaxation and total energy calculation.

The distribution of the structures in the solution space is shown in Fig. 3. In the solution space, the first Pareto front is marked as red. We picked out the structures on the solution space that dominates the defect zinc-blende phase [49] for further calculation. We calculated the bulk modulus by the empirical equation in Eq. (5)

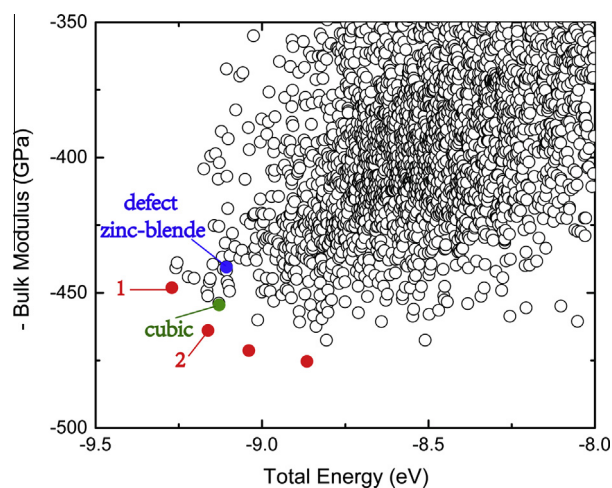


**Fig. 3.** Distribution graph of objectives in the test of C<sub>3</sub>N<sub>4</sub>. Each dot on the objection plane represents a solution generated by IM<sup>2</sup>ODE package. The objection functions are defined in Eq. (5). The red dots highlight the Pareto front of the search results. (For interpretation of the references to colour in this figure legend, the reader is referred to the web version of this article.)

and by fitting the Murnaghan equation of state [51]. Comparing the results in Table 1, we can find out that the value of the empirical equation sometimes differs from that of fitting. The bulk modulus calculated by the empirical equation is strongly related to the bond length, and small change in the bond length will result in great change in it. For the C<sub>3</sub>N<sub>4</sub> system, the bond length of the planer configuration is less than that of the bulk configuration. The

**Table 1**  
The total energy and bulk modulus of cubic C<sub>3</sub>N<sub>4</sub> and those structures that dominates C<sub>3</sub>N<sub>4</sub>.

|                    | Total energy/atom (eV/atom) | $B$ (Eq. (5)) (GPa) | $B$ (ab initio) (GPa) |
|--------------------|-----------------------------|---------------------|-----------------------|
| Defect zinc-blende | 0.0                         | 440.557             | 414.718               |
| Cubic              | −0.022                      | 454.546             | 462.48                |
| 1                  | −0.164                      | 448.134             | 30.859                |
| 2                  | −0.055                      | 463.917             | 140.35                |



structure marked as '1' and '2' in Fig. 3 are partially composed of planer configuration, whose bulk modulus are very large according to the empirical equation but further ab initio calculation gives different result. Therefore further calculation is needed after the searching.

#### 4. Conclusions

In this paper, we introduced a package IM<sup>2</sup>ODE which could be used for inverse design of materials with desired properties. The target properties include the optical and electronic-structure properties of semiconductors, hardness of crystals, etc. For the first time, IM<sup>2</sup>ODE extends the search space of functional materials from single-objective domain to multi-objective domain. Implementing MODE algorithm, IM<sup>2</sup>ODE can explore the complex multi-dimensional solution space efficiently. Therefore IM<sup>2</sup>ODE is able to predict materials with desired properties, which is of great demand in the modern material science. The atomic configurations that can be predicted include three dimensional structure, interface and cluster, even complex defect in solid. We demonstrated the efficiency of the package by some tests on the Al<sub>2</sub>O<sub>3</sub>, C<sub>3</sub>N<sub>4</sub> and carbon phases. Overall, IM<sup>2</sup>ODE is a promising tool for computer-driven material design.

#### Acknowledgement

The authors thank Yang Zhou for completing part of the IM<sup>2</sup>-ODE-package, Zheng-Lu Li for useful discussions on the algorithm, and Shi-Hao Wei for suggestions of the cluster modulation of IM<sup>2</sup>-ODE. Work was supported by NSFC, the Special Funds for Major State Basic Research, Research Program of Shanghai Municipality and MOE, and Program for Professor of Special Appointment (Eastern Scholar). Y.-Y. Zhang thanks the Interdisciplinary Outstanding Doctoral Research Funding of Fudan University.

#### References

- [1] S. Curtarolo, G.L. Hart, M.B. Nardelli, N. Mingo, S. Sanvito, O. Levy, *Nat. Mater.* 12 (2013) 191–201.
- [2] G. Hautier, A. Miglio, G. Ceder, G.M. Rignanese, X. Gonze, *Nat. Commun.* 4 (2013) 2292.
- [3] H. Peng, A. Zakutayev, S. Lany, T.R. Paudel, M. d'Avezac, P.F. Ndione, J.D. Perkins, D.S. Ginley, A.R. Nagaraja, N.H. Perry, T.O. Mason, A. Zunger, *Adv. Funct. Mater.* 23 (2013) 5267–5276.
- [4] J. Carrete, W. Li, N. Mingo, S. Wang, S. Curtarolo, *Phys. Rev. X* 4 (2014) 011019.
- [5] G.L.W. Hart, S. Curtarolo, T.B. Massalski, O. Levy, *Phys. Rev. X* 3 (2013) 041035.
- [6] A. Jain, S.P. Ong, G. Hautier, W. Chen, W.D. Richards, S. Dacek, S. Cholia, D. Gunter, D. Skinner, G. Ceder, K.A. Persson, *APL Mater.* 1 (2013) 011002.
- [7] L. Yu, A. Zunger, *Phys. Rev. Lett.* 108 (2012) 068701.
- [8] A. Franceschetti, A. Zunger, *Nature* 402 (1999) 60–63.
- [9] M. d'Avezac, J.-W. Luo, T. Chanier, A. Zunger, *Phys. Rev. Lett.* 108 (2012) 027401.
- [10] L. Zhang, J.-W. Luo, A. Saraiva, B. Koiller, A. Zunger, *Nat. Commun.* 4 (2013) 2396.
- [11] H.J. Xiang, B. Huang, E. Kan, S.-H. Wei, X.G. Gong, *Phys. Rev. Lett.* 110 (2013) 118702.
- [12] X. Zhang, Y. Wang, J. Lv, C. Zhu, Q. Li, M. Zhang, Q. Li, Y. Ma, J. Chem. Phys. 138 (2013) 114101–114109.
- [13] S.M. Woodley, R. Catlow, *Nat. Mater.* 7 (2008) 937–946.
- [14] Y. Xiang, X. Gong, *Phys. Rev. E* 62 (2000) 4473.
- [15] S. Wu, M. Ji, C. Wang, M. Nguyen, X. Zhao, K. Umamoto, R. Wentzcovitch, K. Ho, *J. Phys. Condens. Matter* 26 (2014) 035402.
- [16] D.J. Wales, H.A. Scheraga, *Science* 285 (1999) 1368–1372.
- [17] C.J. Pickard, R. Needs, *J. Phys. Condens. Matter* 26 (23) (2011) 053201.
- [18] A.R. Oganov, C.W. Glass, *J. Chem. Phys.* 124 (2006) 244704–244715.
- [19] Y. Wang, J. Lv, L. Zhu, Y. Ma, *Comput. Phys. Commun.* 183 (2012) 2063–2070.
- [20] H.A. Abbass, R. Sarker, C. Newton, *Proceedings of the 2001 Congress on Evolutionary Computation*, vol. 972, IEEE, 2001, pp. 971–978.
- [21] F. Xue, A.C. Sanderson, R.J. Graves, *Proceedings of the 2003 Congress on Evolutionary Computation*, vol. 862, IEEE, 2003, pp. 862–869.
- [22] B. Babu, M.M.L. Jehan, in: *Proceedings of the 2003 Congress on Evolutionary Computation*, IEEE, 2003, pp. 2696–2703.
- [23] R. Storn, K. Price, *J. Global Optim.* 11 (1997) 341–359.
- [24] R. Storn, K. Price, *IEEE Conference on Evolutionary Computation*, Nagoya, 1996, pp. 842–844.
- [25] Z. Li, Z. Li, H. Cao, J. Yang, Q. Shu, Y. Zhang, H. Xiang, X.G. Gong, *Nanoscale* (2014).
- [26] Z. Chen, X. Jiang, J. Li, S. Li, L. Wang, *J. Comput. Chem.* 34 (2013) 1046–1059.
- [27] J. Pannetier, J. Bassas-Alsina, J. Rodriguez-Carvajal, V. Caignaert, *Nature* 346 (1990) 343–345.
- [28] C.J. Pickard, R.J. Needs, *J. Chem. Phys.* 127 (2007) 244503–244507.
- [29] Y. Wang, J. Lv, L. Zhu, Y. Ma, *Phys. Rev. B* 82 (2010) 094116.
- [30] X. Luo, J. Yang, H. Liu, X. Wu, Y. Wang, Y. Ma, S.-H. Wei, X. Gong, H. Xiang, *J. Am. Chem. Soc.* 133 (2011) 16285–16290.
- [31] G. Kresse, J. Hafner, *Phys. Rev. B* 49 (1994) 14251–14269.
- [32] H.W. Kuhn, *Nav. Res. Logist. Q* 2 (1955) 83–97.
- [33] R. Joshi, A.C. Sanderson, *IEEE Trans. Syst. Man Cyb. A* 29 (1999) 63–76.
- [34] T. Robič, B. Filipič, *Evolutionary Multi-Criterion Optimization*, Springer, Berlin Heidelberg, 2005, pp. 520–533.
- [35] K.C. Mondal, N. Pasquier, *Biological Knowledge Discovery Handbook: Preprocessing, Mining, and Postprocessing of Biological Data*, John Wiley & Sons, 2014, pp. 761–802.
- [36] A. Zamuda, J. Brest, E. Mezura-Montes, in: *Proceedings of the 2013 Congress on Evolutionary Computation*, IEEE, 2013, pp. 1925–1931.
- [37] K. Deb, A. Pratap, S. Agarwal, T. Meyarivan, *IEEE Trans. Evolut. Comput.* 6 (2002) 182–197.
- [38] H.-Z. Chen, Y.-Y. Zhang, X. Gong, H. Xiang, *J. Phys. Chem. C* 118 (2014) 2333–2337.
- [39] A. Fujishima, K. Honda, *Nature* 238 (1972) 37–38.
- [40] J. Tao, T. Luttrell, M. Batzill, *Nat. Chem.* 3 (2011) 296–300.
- [41] S.U.M. Khan, M. Al-Shahry, W.B. Ingler, *Science* 297 (2002) 2243–2245.
- [42] T. Nikolay, L. Larina, O. Shevaleevskiy, B.T. Ahn, *Energy Environ. Sci.* 4 (2011) 1480–1486.
- [43] M.L. Cohen, *Mat. Sci. Eng. A* 209 (1996) 1–4.
- [44] M. Cohen, *Phys. Rev. B* 32 (1985) 7988–7991.
- [45] D.M. Teter, R.J. Hemley, *Science* 271 (1996) 53–55.
- [46] A.Y. Liu, M.L. Cohen, *Science* 245 (1989) 841–842.
- [47] C. Niu, Y.Z. Lu, C.M. Lieber, *Science* 261 (1993) 334–337.
- [48] A. Liu, M. Cohen, *Phys. Rev. B* 41 (1990) 10727–10734.
- [49] A. Liu, R. Wentzcovitch, *Phys. Rev. B* 50 (1994) 10362–10365.
- [50] M. Khazaei, M.N. Tripathi, Y. Kawazoe, *Phys. Rev. B* 83 (2011).
- [51] F.D. Murnaghan, *Proc. Natl. Acad. Sci. USA* 30 (1944) 244–247.